# Impairment of Photosystem II Donor Side by the Natural Product Odoratol†

Lahoucine Achnine,‡ Rachel Mata,§ Roberto Iglesias-Prieto,|| and Blas Lotina-Hennsen*,‡

Departamento de Bioquímica, Departamento de Farmacia, Facultad de Química, Estación de Investigación Marinas "Puerto Morelos", ICMyL-UNAM, Universidad Nacional Autónoma de México, Mexico, D.F. 04510

The effect of odoratol, a natural protolimonoid, isolated from *Cedrela odorata* (Meliaceae) and two of its derivatives on different photosynthetic reactions of isolated spinach chloroplasts was investigated. This natural product is an inhibitor (150 $\mu$M) of oxygen evolution. Polarographic analyses of the photosynthetic partial redox reactions indicate that (a) photosystem I (PSI) activity is unaffected by odoratol, (b) there is a substantial inhibition of the electron flow of uncoupled photosystem II (PSII) as measured from water to silicomolybdate or diaminodurene, and (c) the electron flow from diphenyl carbazide to dichlorophenolindophenol of Tris-washed chloroplasts was insensitive. Collectively, these data suggest that the site of action of odoratol is located at the donor side of PSII. Comparison of chlorophyll *a* fluorescence induction curves of chloroplasts with authenticated donor side damage and those obtained from odoratol-treated samples further supports this interpretation. Comparative analyses using odoratol derivatives indicate that the diol moiety at positions 23 and 24 of the side chain is an important structural requirement for the inhibitory activity displayed by odoratol.

**Keywords:** *Photosystem II; oxygen evolving complex; odoratol; Cedrela odorata; Meliaceae*

## INTRODUCTION

Photosystem II (PSII) is a supramolecular assemblage anisotropically incorporated into the thylakoid membrane (Debus, 1992). The main function of PSII is to act as a light-driven water−plastoquinone oxidoreductase. PSII can be inactivated by several synthetic or natural compounds. Depending on their targets, these compounds can be regarded as donor or acceptor side inhibitors. In oxygen-evolving photosynthetic organisms the oxidation of water is catalyzed by the manganese cluster located in the oxygen-evolving complex (OEC) at the lumenal side of the thylakoid membrane (Debus, 1992; Ghanotakis and Yocum, 1990). This cluster contains four manganese ions and requires $Cl^-$ and $Ca^{2+}$ as cofactors to function properly (Ghanotakis et al., 1984; Miyao and Murata, 1985). In the literature several compounds and treatments have been reported as OEC inhibitors. For example, depletion of $Ca^{2+}$ and $Cl^-$ from PSII results in reversible inhibition of oxygen evolution while the Mn cluster is retained in its site (Debus, 1992; Homann 1987). Moreover, Tris-washing of thylakoids (Yamashita and Butler, 1968) and hydroxylamine, methylamine, and ammonia treatments induce significant to full inhibition of oxygen evolution in isolated chloroplasts (Joliot, 1966; Izawa and Good, 1972). On the other hand, only few natural compounds have been reported as OEC inhibitors. In this context, we have previously demonstrated that the natural products cacalol and ivalin inhibited oxygen evolution in isolated chloroplasts with $I_{50}$ (concentration producing 50% inhibition) values of 30 $\mu$M and 2.8 mM, respectively (Lotina-Hennsen et al., 1991).

While characterizing the effect of naturally occurring limonoids on several photosynthetic activities, we have discovered the inhibitory effect of odoratol, a protolimonoid isolated from *Cedrela odorata* (Meliaceae), on the donor side of PSII of isolated spinach chloroplasts. In this paper, we discuss the evidence of the inhibitory properties of odoratol based on two different techniques, namely oxymetry and chlorophyll *a* (Chl *a*) fluorescence measurements.

## MATERIALS AND METHODS

**Procedures for the Preparation of Odoratol and Its Derivatives.** Odoratol was obtained from a $CHCl_3$/methanolic extract (1:1) of *C. odorata* L. (Meliaceae) wood. The structure of this natural product was established using spectrometric and spectroscopic (IR and NMR) methods (Chan et al., 1968). Odoratol (**1**) afforded triacetate (**2**) upon treatment with acetic anhydride and pyridine. Treatment of odoratol (**1**) with acetone and catalytic amounts of hydrochloric acid at room temperature readily gave the corresponding acetonide (**3**) (Figure 1). Derivatives **2** and **3** were also characterized by spectral and spectroscopic means.

**Biological Activities.** Chloroplasts were obtained from spinach leaves (*Spinacea oleraceae* L.) as described earlier (Lotina-Hennsen et al., 1987). The chlorophyll concentration was measured spectrophotometrically as reported (Strain et al., 1971). Proton uptake was measured as the pH rise between 8.0 and 8.1 (Dilley, 1972). Photophosphorylation was measured as proton uptake conditions, in the presence of 1 mM ADP and 3 mM $KH_2PO_4$ (Lotina-Hennsen et al., 1987). KCN (100 $\mu$M) was added to inhibit catalase activity. Electron flows (basal, phosphorylating, and uncoupled) from water to methyl viologen (MV) were determined according to the procedures previously described (Lotina-Hennsen et al., 1991). Partial reactions of the electron transport chain were mea-

* Author to whom correspondence should be addressed (e-mail blas@servidor.unam.mx; fax +52 5 622 53 29).

† This work was taken in part from the Ph.D. thesis of L.A.

‡ Departamento de Bioquímica.

§ Departamento de Farmacia.

|| Estación de Investigaciones Marinas.

10.1021/jf980589+ CCC: $15.00 
Published on Web 11/12/1998

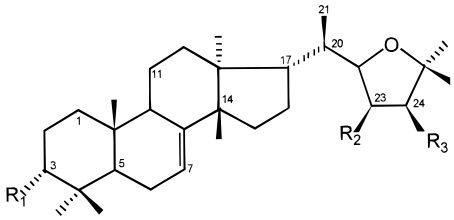

**1** $R_1 = R_2 = R_3 =$ OH
**2** $R_1 = R_2 = R_3 =$ OAc
**3** $R_1 =$ OH $R_2, R_3 =$ 

**Figure 1.** Structures of odoratol (**1**), triacetylodoratol (**2**), and odoratol acetonide (**3**).

sured using specific inhibitors, 3-(3,4-dichlorophenyl)-1,1-dimethylurea (DCMU; 10 $\mu$M) and 2,5-dibromo-3-methyl-6-isopropyl-*p*-benzoquinone (DBMIB; 1 $\mu$M), and the following electron donors and acceptors: silicomolybdate (SiMo; 100 $\mu$M); dichlorophenol indophenol (DCPIP; 100 $\mu$M); diphenyl carbazide (DPC; 200 $\mu$M); diaminodurene (DAD; 100 $\mu$M); and MV (100 $\mu$M) (Allen and Holmes, 1986).

To monitor Chl *a* fluorescence transients, induction aliquots of dark-adapted chloroplasts containing 15 $\mu$g of chlorophyll were transferred to filter paper by gravity and immediately dipped in 3 mL of different concentrations of the tested compounds. Samples were incubated for 5 min in the dark. Chl *a* fluorescence induction curves were measured at room temperature by a portable shutterless apparatus (Plant Efficiency Analyzer, Hansatech, U.K.) described previously (Strasser et al., 1995). Excitation was provided by an array of six light-emitting diodes delivering 600 W·m$^{-2}$ of red light (peak at 650 nm). Samples infiltrated with hydroxylamine were washed in the dark several times with fresh isolation buffer before been assayed. Ethylenediaminetetraacetic acid (EDTA) was present to chelate Mn(II) ions released from the $O_2$-evolving center. Kinetic analyses of the relative variable fluorescence were performed by deconvolution of data collected during the first 2 ms with 10 $\mu$s resolution. Deconvolution analyses were performed with a nonlinear fitting procedure.

## RESULTS AND DISCUSSION

**Effect of Odoratol on Photosynthetic Activities.** Odoratol (150 $\mu$M) inhibited ATP formation and $H^+$-uptake by 96.3 and 89.9%, respectively (Figure 2) with $I_{50}$ of 35 $\mu$M. The light-dependent synthesis of ATP and $H^+$-uptake by illuminated thylakoids might be inhibited in a number of ways: (a) by uncoupling ATP synthesis from the electron transport, (b) by blocking the electron transport, and/or (c) by blocking the phosphorylation reaction itself. To understand the mechanism by which odoratol inhibited the photophosphorylation, its effect on the electron transport chain was investigated. Odoratol (150 $\mu$M) inhibited basal, phosphorylating, and uncoupled electron transports by 87.7, 85.5, and 78.8%, respectively (Figure 2). Therefore, this protolimonoid behaves as Hill reaction inhibitors.

To localize the inhibition site of odoratol, its effect on photosystem I (PSI) and PSII electron transports was evaluated. PSI activity, measured from DCPIP/$H_2$ to MV, was insensitive to odoratol. However, the natural product (150 $\mu$M) inhibited the electron flow through PSII, measured from water to DCPIP, by 86.6% (Figure 3). The p$I_{50}$ value for PSII inhibition was 4.6. Thus, the level of activity displayed by odoratol as PSII inhibitor is comparable with that of good PSII inhibitors, which possess p$I_{50}$ values in the range of 6−7 (Bowyer et al., 1991). To further determine the target of odoratol, the partial reactions of PSII were studied: the uncoupled PSII electron flows (5 mM $NH_4Cl$) from water to SiMo and from $H_2O$ to DAD were inhibited by 88.7 and 90.8%, respectively, at 150 $\mu$M. However, the electron flow from DPC to DCPIP of 0.8 M Tris-washed chloroplasts was unaffected by odoratol (Figure 3). It is known that DPC is an electron donor to PSII (Vernon and Shaw, 1969). This reaction is dependent on the DPC concentration, the pH of the medium, and the integrity of the thylakoid membranes. Consequently, compound **1** behaves as a water-splitting enzyme inhibitor. Therefore, odoratol acts at the same target as cacalol and ivalin do (Lotina-Hennsen et al., 1991; Bernal-Morales et al., 1994)

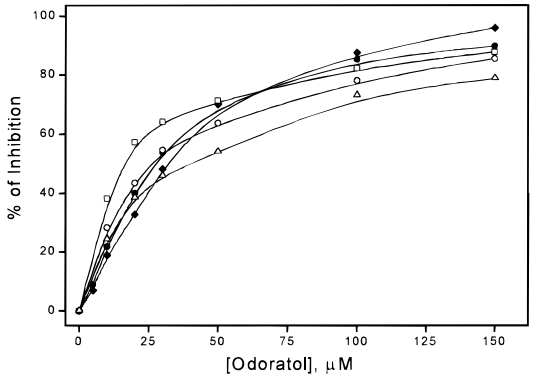


**Figure 2.** Effect of increasing concentrations of odoratol on photophosphorylation (◆), $H^+$-uptake (●), basal (□), phosphorylating (○), and uncoupled (△) electron transports from water to methyl viologen in intact spinach chloroplasts. Control rate values for ATP synthesis and $H^+$-uptake were 350 and 280 $\mu$mol/(h·mg of Chl), respectively. Control rate values for basal, phosphorylating, and uncoupled electron transport were 380, 560, and 840 $\mu$equiv e$^-$/(h·mg of Chl), respectively.

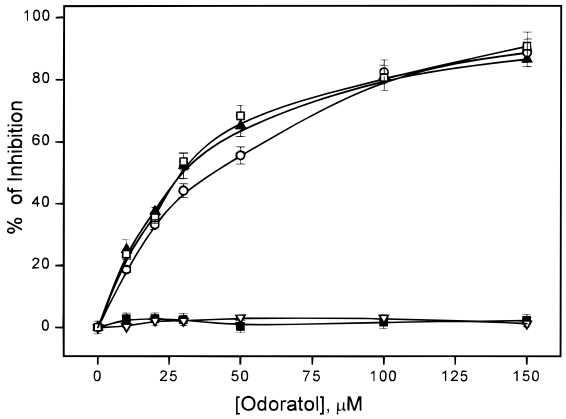


**Figure 3.** Electron transport through uncoupled photosystem I (■) and photosystem II (▲), from water to SiMo (○), from water to DAD (□), and from DPC to DCPIP (▽) as a function of increasing concentrations of odoratol. Control rate values for these electron flows were 910, 980, 250, 650, and 210 $\mu$equiv e$^-$/(h·mg of Chl), respectively.

To find out the influence of the carbinol groups present in the molecule of odoratol in the different photosynthetic activities tested, the effect of two odoratol derivatives (triacetyl derivative **2** and odoratol acetonide **3**) on the same photosynthetic reactions was also investigated. Compounds **2** and **3** did not show appreciable activity in comparison to odoratol. On the other hand, the hydroxyl moiety at position 3 did not enhance the activity of odoratol (Table 1). Thus, the two vicinal OH groups at positions 23 and 24 of odoratol

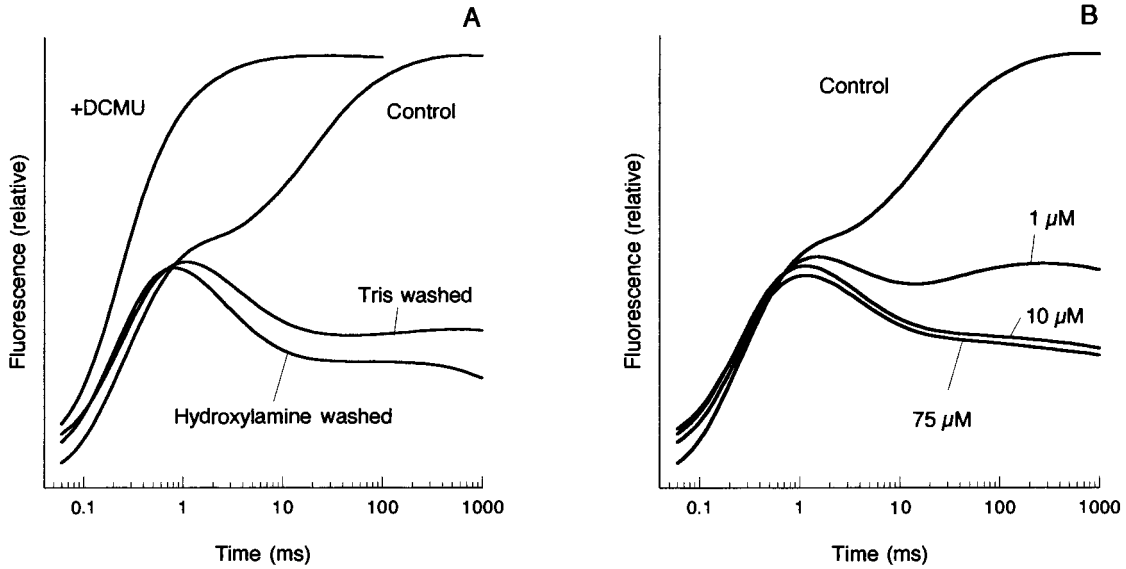


**Figure 4.** (A) Fluorescence induction curves of control chloroplasts and authenticated samples with acceptor side damage (+DCMU) and donor side impairment (Tris and hydroxylamine). (B) Chlorophyll fluorescence induction curves of controls and samples infiltrated with different concentrations of odoratol.

**Table 1. Effect of Odoratol and Its Derivatives on Uncoupled PSII Electron Transport from Water to DAD, from Water to SiMo, and from DPC to DCPIP[a]**

| | % inhibition | | |
|---|---|---|---|
| addition | $H_2O$ to DAD | $H_2O$ to SiMo | DPC to DCPIP |
| odoratol | | | |
| none | 0 | 0 | 0 |
| 10 μM | 23.6 | 18.4 | 0.7 |
| 50 μM | 68.4 | 55.3 | 1.0 |
| 100 μM | 80.7 | 76.6 | 0.8 |
| 150 μM | 90.8 | 88.7 | 1.2 |
| triacetylodoratol | | | |
| none | 0 | 0 | 0 |
| 50 μM | 4.1 | 1.7 | 2.5 |
| 100 μM | 6.4 | 5.3 | 6.4 |
| 200 μM | 8.1 | 10.2 | 12.4 |
| 500 μM | 9.5 | 12.5 | 14.2 |
| odoratol acetonide | | | |
| none | 0 | 0 | 0 |
| 50 μM | 2.5 | 4.3 | 3.5 |
| 100 μM | 8.4 | 9.4 | 8.5 |
| 200 μM | 10.3 | 13.5 | 12.4 |
| 500 μM | 13.4 | 16.5 | 15.6 |

[a] Control values for these electron flows were 650, 250, and 210 μequiv $e^-$/(h·mg of Chl), respectively.

are essential for the displayed inhibitory interaction of the natural product with the OEC.

**Chl *a* Fluorescence Evidence of the PSII Donor Side Impairment.** Isolated spinach chloroplasts show a polyphasic fluorescence curve with regular O−J−I−P sequence of transients similar to those previously described for several intact organisms (Iglesias-Prieto, 1995; Srivastava et al., 1995). The OJIP sequence represents the successive reduction of the electron acceptor pool of PSII (Govindjee, 1995). Chloroplasts infiltrated with several authenticated PSII inhibitors show dramatic changes in their fluorescence induction curves (Figure 4A). Variations in the fluorescence induction signatures are dependent on the site of action of the authenticated inhibitors. Inactivation of the PSII acceptor side after the addition of DCMU resulted in the loss of the regular OJIP sequence and the formation of an OJ sequence. Addition of Tris and hydroxylamine, two well-known donor side inhibitors of PSII (Britt, 1996), resulted in the formation of a faster fluorescence transient at ∼0.8 ms, followed by reduction in the fluorescence yield (Figure 4A). This event appears to be consistent with transient K recently described in green plants under severe thermal stress (Guissé et al., 1995). Transient K probably originates from the increase of the lifetime of the $P_{680}^+$ and $Phe^-$ radical pair due to limitations in the electron supply from the OEC. Losses of variable fluorescence after 0.8 ms are consistent with the increase in $P_{680}^+$ lifetime as this radical is an efficient fluorescence quencher (Krause and Weis, 1984). Comparison of the fluorescence induction curves of chloroplasts infiltrated with inhibitors of the OEC (Tris, $NH_2OH$) with those obtained from chloroplasts exposed to different concentrations of odoratol clearly shows remarkable similarities (Figure 4). As in the case of authenticated controls with donor side impairment, exposure to odoratol resulted in the formation of transient K, followed by a reduction of variable fluorescence.

Analyses of the changes in relative variable fluorescence yield $[V(t) = (F_t - F_0)/(F_m - F_0)]$ during the first 2 ms of the induction curve provide us with a detailed description of the kinetic responses of PSII to different inhibitors. The rise of $V(t)$ in control chloroplasts requires two components to be accurately described (Figure 5A). A fast sigmoidal component with a rate constant of ∼0.10 $ms^{-1}$ and a slow exponential one with a time constant of ∼0.4 $ms^{-1}$ (Table 2; Figure 5A). In contrast, in chloroplasts with donor side impairment a third exponential negative component is required to describe the loss of $V(t)$ after 0.8 ms. For consistency, we employed here three components to deconvolute the initial part of the induction curve (Figure 5A,B). The exponential phase data reported here were obtained by the subtraction of the positive and negative components.

Probably, the most dramatic response of the fluorescence induction curve to donor side inactivation of PSII is the increase in the initial rates of photochemistry ($dV/dt_0$) (Figure 5A,B). Kinetic analyses of induction curves revealed that acceptor side inactivation of PSII produced by infiltration with DCMU resulted in increases in the amplitude of both exponential and sigmoidal components without any significant changes in their rate constants relative to control chloroplasts (Table 2). In

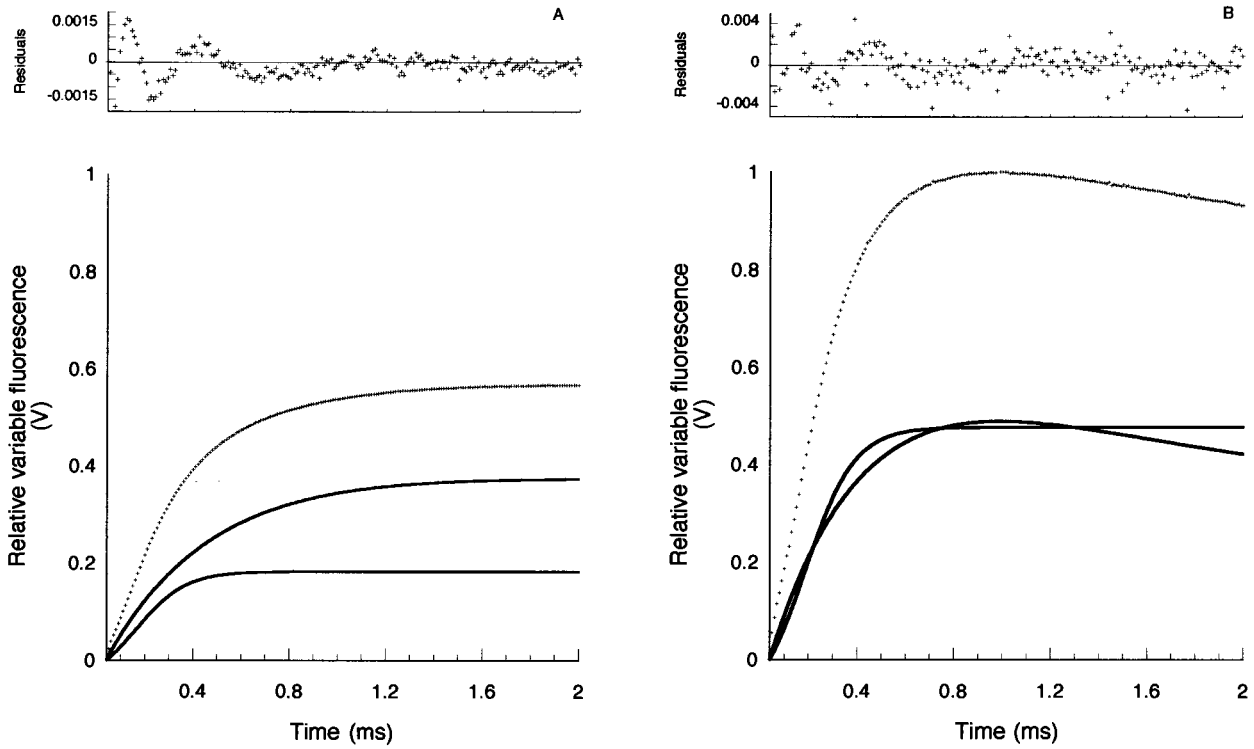


**Figure 5.** (A) Time-dependent variations in the relative variable fluorescence of control chloroplasts. Solid lines represent the exponential and sigmoidal components required to explain the empirically obtained fluorescence data (crosses). (B) Deconvolution of normalized fluorescence curves of chloroplasts infiltrated with 75 $\mu$M odoratol. In both cases upper panels represent the distribution of residuals.

**Table 2. Comparative Kinetic Analyses of the First 2 ms of the Chl *a* Fluorescence Induction Curves of Samples with Authenticated Donor and Acceptor Side Inhibition and Those Infiltrated with Different Concentrations of Odoratol**

| | component | | | | |
|---|---|---|---|---|---|
| | sigmoidal | | | exponential | |
| treatment | amplitude (relative) | sigmoidicity (relative) | rate constant ($ms^{-1}$) | amplitude (relative) | rate constant ($ms^{-1}$) |
| control | 0.2326 | 0.1702 | 0.1008 | 0.411 | 0.3801 |
| DCMU | 0.4726 | 0.1268 | 0.0986 | 0.5221 | 0.4065 |
| Tris | 0.5877 | 0.1873 | 0.1007 | 0.4218 | 0.0550 |
| $NH_2OH$ | 0.7561 | 0.1499 | 0.0959 | 0.2120 | 0.0913 |
| odoratol | | | | | |
| 1 $\mu$M | 0.4523 | 0.2001 | 0.1052 | 0.5700 | 0.1887 |
| 10 $\mu$M | 0.6774 | 0.1728 | 0.1095 | 0.3652 | 0.1303 |
| 75 $\mu$M | 0.6283 | 0.1642 | 0.1090 | 0.4262 | 0.0753 |

contrast, comparison of the kinetic characteristics of authenticated samples with donor side damage and those obtained from control chloroplasts indicates that the increase in $dV/dt_0$ resulted from a decrease in the rate constant of the exponential component (Table 2). The results show no detectable variation in the rate constants or in the connectivity of the sigmoidal components of chloroplasts with donor side damage relative to controls. Similar to the results obtained for the authenticated samples, addition of odoratol produces sequentially similar increases in the rate constant of the exponential component without variation in the kinetics of the sigmoidal one.

**Concluding Remarks.** The analyses of the fluorescence signatures of donor side damage of chloroplasts are consistent with the polarographic evidence presented here and strongly suggest that the site of action of odoratol is located at the donor side of PSII. Therefore, the use of this simple chlorophyll fluorescence technique probably will have a great potential to screen a large variety of synthetic and natural compounds with herbicide potential.

This work is intended to be part of a much larger survey of the effects of naturally occurring compounds, including limonoids from the Meliaceae family, on various plant processes to improve understanding of the interaction between plants through the so-called allelochemical compounds.

## ABBREVIATIONS USED

Chl *a*, chlorophyll *a*; DAD, diaminodurene; DBMIB, 2,5-dibromo-3-methyl-6-isopropyl-*p*-benzoquinone; DCMU, 3-(3,4-dichlorophenyl)-1,1-dimethylurea; DCPIP, dichlorophenol indophenol; DPC; diphenyl carbazide; EDTA, ethylenediaminetetraacetic acid; SiMo, silicomolybdate; MV, methyl viologen; OEC, oxygen evolving complex; PSII, photosystem II; PSI, photosystem I.

## LITERATURE CITED

Allen, J. F.; Holmes, N. G. Electron transport and redox titration. In *Photosynthesis, Energy Transduction: A Practical Approach*; Hipkins, M. F., Baker, N. R., Eds.; IRL Press: Oxford, U.K., 1986; Chapter 5, pp 103−141.

Bernal-Morales, E.; Romo De Vivar, A.; Sánchez, B.; Aguilar, M.; Lotina-Hennsen, B. Inhibition of oxygen evolution by ivalin. *Can. J. Bot.* **1994**, *72*, 177−181.

Bowyer, J. R.; Camilleri, P.; Vermaas, W. F. J. Photosystem II and its interaction with herbicides. In *Herbicides*; Baker, N. R., Percival, M. P., Eds.; Elsevier Science Publishers: Amsterdam, 1991; pp 27−79.

Britt, R. D. Oxygen evolution. In *Advances in Photosynthesis: Oxygenic Photosynthesis: The Light Reactions*; Ort, D. R., Yocum, C. F., Eds.; Kluwer Academic Publishers: Amsterdam, 1996; Vol. V, pp 137−164.

Chan, W. R.; Holder, N. L.; Snatzke, G.; Fehlhaber, H. W.; Taylor, D. R. Extractives of *Cedrela odorata*. II. The structures of *Cedrela* tetracyclic triterpenes odoratol, isoodoratol and odoratone. *J. Chem. Soc. C* **1968**, *20*, 2485−2489.

Debus, R. The manganese and calcium ions of photosynthetic oxygen evolution. *Biochim. Biophys. Acta* **1992**, *1102*, 269−352.

Dilley, R. A. Ion transport ($H^+$, $K^+$, $Mg^{2+}$ exchange phenomena). In *Methods in Enzymology*; San Pietro, A., Ed.; Academic Press: New York, 1972; Vol. 24, Section I, Methodology, pp 68−74.

Ghanotakis, D. F.; Yocum, C. F. Photosystem II and the oxygen evolving complex. *Annu. Rev. Plant Physiol. Mol. Biol.* **1990**, *41*, 155−276.

Ghanotakis, D. F.; Babcock, G. T.; Yocum, C. F. Calcium reconstitutes high rates of oxygen evolution in polypeptide depleted photosystem II preparations. *FEBS Lett.* **1984**, *167*, 127−130.

Govindjee. Sixty-three years since Kautsky: chlorophyll *a* fluorescence. *Aust. J. Plant Physiol.* **1995**, *22*, 131−160.

Guissé, B.; Srivastava, A.; Strasser, R. J. Effects of high temperature and water stress on the polyphasic chlorophyll *a* fluorescence transient of potato leaves. In *Photosynthesis: from Light to Biosphere*; Mathis, P., Ed.; Kluwer: Dordrecht, 1995; Vol. IV, pp 913−916.

Homann, P. H. The relation between the chloride, calcium, and plypeptide requirements of photosysthetic water oxidation. *J. Bioenerg. Biomembr.* **1987**, *19*, 105−123.

Iglesias-Prieto, R. The effects of elevated temperature on the photosynthetic responses of symbiotic dinoflagellates. In *Photosynthesis: from Light to Biosphere*; Mathis, P., Ed.; Kluwer: Dordrecht, 1995; Vol. IV, pp 793−796.

Izawa, S.; Good, N. E. Inhibition of photosynthetic electron transport and photophosphorylation. In *Methods in Enzymology*; San Pietro, A., Ed.; Academic Press: New York, 1972; Vol. 24, Part B, pp 355−377.

Krause, G. H.; Weis, E. Chlorophyll fluorescence as a tool in plant physiology. II Interpretation of fluorescence signals. *Photosynth. Res.* **1984**, *5*, 139−157.

Lotina-Hennsen, B.; King, B.; Albores, M.; Pozas, R. Uncoupling of photophosphorylation by nitrogenous bases. No correlation of uncoupling with pKb and partition coefficient. *Photochem. Photobiol.* **1987**, *46*, 287−293.

Lotina-Hennsen, B.; Roque-Reséndiz, J. L.; Jiménez, M.; Aguilar, M. Inhibition of oxygen evolution by cacalol and its derivatives. *Z. Naturforsch.* **1991**, *46C*, 777−780.

Miyao, M.; Joliot, A. Actions du chloromethylurée et de l'hydroxylamine sur la réaction photochimique d'émission d'oxygène (système II). *Biochim. Biophys. Acta* **1966**, *126*, 587−593.

Miyao, M.; Murata, N. The $Cl^-$ effect on photosynthetic oxygen evolution: interaction of $Cl^-$ with 18-kDa, 24-kDa and 33-kDa proteins. *FEBS Lett.* **1985**, *180*, 303−308.

Murata, N. The $Cl^-$ effect on photosynthetic oxygen evolution: Interaction of $Cl^-$ with 18-kDa, 24 kDa and 33-kDa proteins. *FEBS Lett.* **1985**, *180*, 303−308.

Srivastava, A.; Strasser, R. J.; Govindjee. Polyphasic rise of chlorophyll *a* fluorescence in herbicide-resistant D1 mutants of *Chlamydomonas reinardtii*. *Photosynth. Res.* **1995**, *43*, 131−141.

Strain, H. H.; Cope, T.; Svec, M. A. Analytical procedures for the isolation, identification, estimation and investigation of the chlorophylls. *Methods Enzymol.* **1971**, *23*, 452−466.

Strasser, R. J.; Srivastava, A.; Govindjee. Polyphasic chlorophyll *a* fluorescence transient in plants and cyanobacteria. *Photochem. Photobiol.* **1995**, *61*, 32−42.

Vernon, L. P.; Shaw, E. R. Photoreduction of 2,6-dichlorophenolindophenol by diphenylcarbazide: a photosystem II reaction catalyzed by Tris-washed chloroplast and subchloroplast fragments. *Plant Physiol.* **1969**, *44*, 1645−1649.

Yamashita, T.; Butler, W. L. Photoreduction and phosphorylation with Tris-washed chloroplasts. *Plant Physiol.* **1968**, *43*, 1978−1984.

Received for review June 3, 1998. Revised manuscript received September 23, 1998. Accepted September 23, 1998. This work was supported by Grant IN205197 from DGAPA, UNAM; Grants 005341 and 202335 from PADEP, UNAM; and Grant 400313-5-2358PN from CONACyT. L.A. acknowledges the fellowship awarded by DGEP, UNAM, to carry out his graduate studies.

JF980589+